Supplemental Material for: "Electronic structure and phase stability of oxide semiconductors: performance of dielectric-dependent hybrid functional DFT, benchmarked against GW bandstructure calculations and experiments"

Matteo Gerosa
Department of Energy, Politecnico di Milano, via Ponzio 34/3, 20133 Milano, Italy

Carlo Enrico Bottani
Department of Energy, Politecnico di Milano, via Ponzio 34/3, 20133 Milano, Italy and
Center for Nano Science and Technology @Polimi,
Istituto Italiano di Tecnologia, via Pascoli 70/3, 20133 Milano, Italy

Lucia Caramella and Giovanni Onida
Dipartimento di Fisica, Università degli Studi di Milano, Milano, Italy and
European Theoretical Spectroscopy Facility (ETSF)

Cristiana Di Valentin and Gianfranco Pacchioni
Dipartimento di Scienza dei Materiali, Università di Milano-Bicocca, via R. Cozzi 53, 20125 Milan, Italy

(Dated: January 27, 2015)

I. HYBRID DFT AND GW: COMPUTATIONAL DETAILS

As discussed in the main text, DFT hybrid functional calculations can be very expensive using a plane-waves (PW) basis set. In particular, the computational effort strongly depends on the choice of the Brillouin-zone (BZ) sampling. This is illustrated in Fig. S1 for the test case of MgO.

In Table S1 we report k- and q-point grids of our PW calculations performed with the QUANTUM ESPRESSO package. In total energy calculations using the CRYSTAL09 code, convergence studies on the BZ sampling were carried out so as to ensure accuracy within 1 meV on total energies for the various phases. This corresponds to 10x10x10 for MgO, and at least 14x14x14 for ZnO, 6x6x6 for TiO_2, 6x6x6 for ZrO_2, and 4x4x4 for WO_3.

Table S2 collects various cutoff parameters entering GW calculations for the materials investigated in Section III A of the main text. The meaning of the single cutoff parameters is discussed in Section II C of the main text.

TABLE S1: Computational parameters of DFT PW calculations: k- and q-point BZ sampling and PW kinetic energy cutoff $E_{\rm cut}$ (in Ry).

	k-point grid	q-point grid	$E_{\rm cut}$
MgO	4x4x4	4x4x4	500
ZnO	4x4x2	4x4x2	300
TiO_2	4x4x2	4x4x2	150
ZrO_2	4x4x4	4x4x4	120
WO_3	2x2x2	2x2x2	100

TABLE S2: Computational cutoff parameters used in GW calculations: cutoff energies $E^{\rm eps}_{\rm cut}$ and $E^{\rm xc}_{\rm cut}$ (in Ry) controlling the size of the dielectric matrix in reciprocal space and the number of plane waves in the expansion of xc potential, respectively; number of empty states included in the evaluation of the polarizability χ and of the Coulomb hole (CH) term.

			Empty states	
	$E^{\rm eps}_{\rm cut}$	$E^{\rm xc}_{\rm cut}$	χ	$\Sigma_{\rm CH}$
MgO	90	80	300	900
ZnO	70	200	200	2750
TiO_2	14	50	500	1300
ZrO_2	25	50	500	2100
WO_3	16	60	800	2300

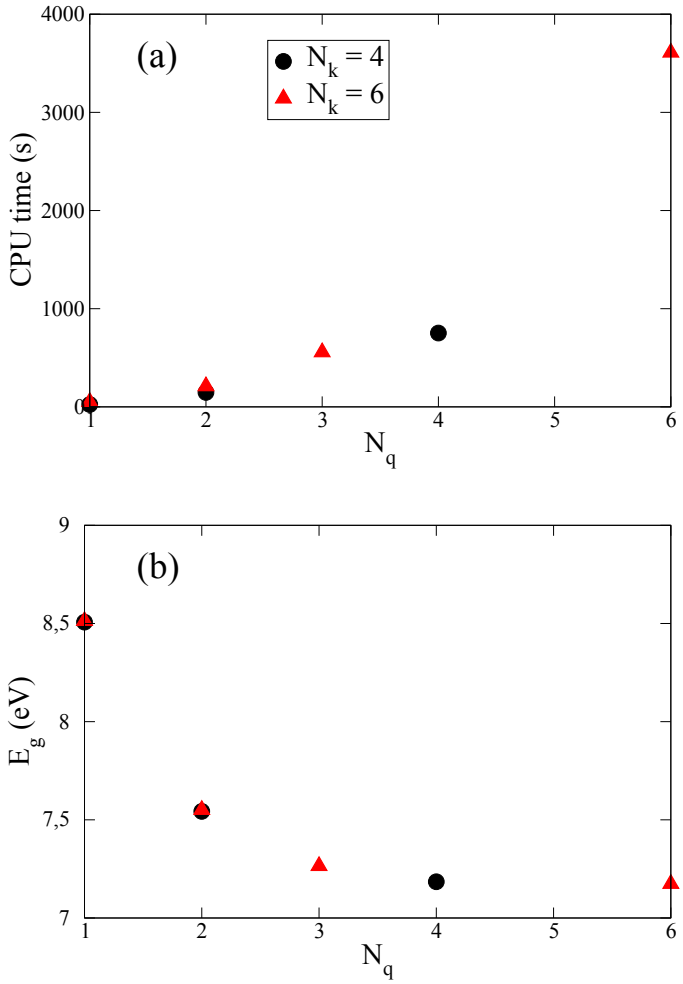

FIG. S1: (a) CPU time and (b) band gap of MgO in hybrid PBE0 calculations with QUANTUM ESPRESSO, using k- and q-point grids of different sizes; N_k and N_q indicate, respectively, $N_k \times N_k \times N_k$ and $N_q \times N_q \times N_q$ Monkhorst-Pack grids.

II. LATTICE PARAMETERS

In Table S3 we report experimental lattice constants used in all the relevant calculations presented in the main text (see Section III A), together with the results of the geometry optimizations performed within LDA and PBE with QUANTUM ESPRESSO for the purpose of validating pseudopotentials. The tendency of LDA and GGA to underestimate and overestimate, respectively, lattice constants is confirmed by our calculations.

Results of geometry optimizations carried out with CRYSTAL09 for the phases not included in Table VII of the main text are reported in Table S4. Calculations were carried out within PBE, PBE0 and dielectric-dependent PBE0, PBE0$\alpha^{(1)}_{\rm PBE}$.

TABLE S3: Lattice constants computed within LDA and PBE with QUANTUM ESPRESSO, and comparison with experiments.

	Type	Parameter	LDA	PBE	Expt.[a]
MgO	rocksalt	a (Å)	4.156	4.230	4.212
ZnO	wurtzite	a (Å)	3.172	3.242	3.249
		c (Å)	5.113	5.215	5.207
		u	0.379	0.380	0.382
TiO_2	anatase	a (Å)	3.748	3.795	3.781
		c (Å)	9.427	9.645	9.515
		u	0.209	0.207	0.208
ZrO_2	tetragonal	a (Å)	3.559	3.613	3.571
		c (Å)	5.116	5.268	5.182
		d_z	0.0434	0.0566	0.0574
WO_3	γ-monoclinic	a (Å)	7.325	7.437	7.306
		b (Å)	7.477	7.683	7.540
		c (Å)	7.557	7.777	7.692
		β (°)	90.98	90.10	90.88

[a]Experimental lattice constants are found in the following references: Ref. 1 for MgO, Ref. 2 for ZnO, Ref. 3 for TiO_2, Ref. 4 for ZrO_2, Ref. 5 for WO_3.

TABLE S4: Optimized cell parameters for selected polymorphs of the studied materials, computed at different levels of theory with CRYSTAL09.

	Type	Parameter	PBE	PBE0	PBE0$\alpha^{(1)}_{\rm PBE}$	Expt.[a]
ZnO	zinc-blende	a (Å)	4.584	4.547	4.541	4.620
TiO_2	rutile	a (Å)	4.621	4.568	4.588	4.587
		c (Å)	3.002	2.978	2.987	2.954
	brookite	a (Å)	9.260	9.177	9.201	9.174
		b (Å)	5.518	5.441	5.464	5.449
		c (Å)	5.215	5.156	5.176	5.138
	cubic	a (Å)	5.148	5.103	5.112	5.110
ZrO_2	monoclinic	a (Å)	5.224	5.189	5.192	5.151
		b (Å)	5.293	5.246	5.253	5.212
		c (Å)	5.382	5.330	5.334	5.317
		β (°)	99.57	99.51	99.51	99.23
	cubic	a (Å)	3.834	3.786	3.811	3.772
	tetragonal	a (Å)	5.345	5.281	5.295	5.250
		c (Å)	4.058	4.018	4.031	3.915
	ε-monoclinic	a (Å)	5.532	5.286	5.295	5.277
		b (Å)	5.259	5.193	5.202	5.155
		c (Å)	7.880	7.794	7.805	7.663
		β (°)	91.16	91.18	91.19	91.76
WO_3	triclinic	a (Å)	7.430	7.334	7.343	7.313
		b (Å)	7.658	7.592	7.619	7.525
		c (Å)	7.854	7.781	7.799	7.689
		α (°)	89.21	89.23	89.28	88.85
		β (°)	90.61	90.55	90.52	90.91
		γ (°)	90.72	90.64	90.60	90.94
	orthorombic	a (Å)	7.518	7.419	7.430	7.341
		b (Å)	7.779	7.705	7.715	7.570
		c (Å)	7.926	7.848	7.859	7.754

[a]Experimental lattice constants are found in the following references: Ref. 6 for zinc-blende ZnO; Refs. 7,8 for rutile and brookite TiO_2; Refs. 9,10 for cubic and monoclinic ZrO_2; Refs. 11–15 for cubic, tetragonal, low-temperature ε-monoclinic. triclinic and orthorombic WO_3.

[1] D. R. Lide (CRC Press/Taylor and Francis, Boca Raton, FL, 1998/1999), 79th ed.

[2] D. F. Croxall, R. C. C. Ward, C. A. Wallace, and R. C. Kell, J. Cryst. Growth **22**, 117 (1974).

[3] M. Horn, C. F. Schwerdtfeger, and E. P. Meagher, Z. Kristallogr. **136**, 273 (1972).

[4] E. V. Stefanovich, A. L. Shluger, and C. R. A. Catlow, Phys. Rev. B **49**, 11560 (1994).

[5] B. O. Loopstra and H. M. Rietveld, Acta Crystallogr., Sect. B **25**, 1420 (1969).

[6] W. H. Bragg and J. A. Darbyshire, J. Met. **6**, 238 (1954).

[7] R. J. Swope, J. R. Smyth, and A. C. Larson, Am. Mineral. **80**, 448 (1995).

[8] E. P. Meagher and G. A. Lager, Can. Mineral. **17**, 77 (1979).

[9] R. P. Ingel and D. Lewis, J. Am. Ceram. Soc. **69**, 325 (1986).

[10] C. J. Howard, R. J. Hill, and B. E. Reichert, Acta Crystallogr., Sect. B **44**, 116 (1988).

[11] W. A. Crichton, P. Bouvier, and A. Grzechnik, Mater. Res. Bull. **38**, 289 (2003).

[12] W. L. Kehl, R. G. Hay, and D. Wahl, J. Appl. Phys. **23**, 212 (1952).

[13] E. K. H. Salje, S. Rehmann, F. Pobell, D. Morris, K. S. Knight, T. Herrmannsdörfer, and M. T. Dove, J. Phys.: Condens. Matter **9**, 6564 (1997).

[14] P. M. Woodward, A. W. Sleight, and T. Vogt, J. Phys. Chem. Solids **56**, 1255 (1995).

[15] E. Salje, Acta Crystallogr., Sect. B **33**, 574 (1977).